# Microwave Induced Plasma Time-of-Flight Mass Spectrometry (mipTOF) for Real-Time Analysis of Metal-Containing Aerosols

Alex Gundlach-Graham, Carsten Stoermer, and Martin Tanner
TOFWERK, Switzerland

## Introduction

Metal-containing aerosols are widely distributed throughout Earth's atmosphere, originating from both natural and anthropogenic sources. These range from mineral dust and volcanic emissions to human activities such as industrial processes, fossil fuel combustion, and vehicular emissions. The varied sources and environmental significance of these metallic particles make their precise measurement crucial for understanding atmospheric chemistry and air quality. These metals are present across a concentration range of more than ten orders of magnitude, from ~10-6 to 100,000 ng/m3 [1], and are highly dependent on local environmental factors, including proximity to emission sources and wind velocity [2].

## Current Measurement Technologies and Limitations

Conventionally, the concentrations of metal aerosols are determined via particle collection on a filter followed by total digestion and bulk analysis with inductively coupled plasma mass spectrometry (ICP-MS) [3]. However, the time resolution of bulk analysis (around 24 hours) limits the utility of source apportionment and precludes co-variation analysis and/or data fusion of metal aerosol concentration data with highly time resolved organic aerosol analyses, e.g. from proton transfer reaction time-of-flight mass spectrometry (PTR-TOFMS) or aerosol mass spectrometry (AMS) [4-6].

In recent years, field portable X-ray Fluorescence (XRF) instruments have gained more widespread use in research and air quality monitoring (AQM) applications [7]. These instruments can provide bulk concentrations of metal aerosols with improved time resolution (ca. 60 min), albeit with reduced sensitivity compared to traditional collect-and-digest ICP-MS analyses. While an improvement, the time resolution offered by field portable XRF still is insufficient for accurate source apportionment analysis because

data at this time scale cannot intrinsically account for environmental factors such as wind velocity.

Single-particle aerosol mass spectrometry (SPMS) [8] and real-time mass spectrometry of volatile organic compounds (VOCs), e.g. via PTR-MS [9], are broadly used approaches in atmospheric research and AQM. These instruments provide high-sensitivity ambient air measurements on a timescale of seconds. At this time resolution, wind-velocity-resolved data can be generated, which greatly improves source apportionment analyses. In addition, mobile measurements to localize aerosol events in time and space are possible [10]. Advancements in real-time MS analysis of ambient air have revolutionized AQM and provide a means to detect and enforce air pollution regulations. However, to date, comparable instrumentation for the real-time quantitative analysis of metal containing aerosols has not emerged.

Here, we report the development of a new trace-element mass spectrometer for the direct quantitative analysis of metals in ambient air. This microwave induced plasma time-of-flight mass spectrometer (mipTOF) features a nitrogen ($N_2$) sustained plasma source [11, 12] that can be used to continuously and directly vaporize, atomize, and ionize metals and metalloids from aerosol particles in ambient air. Together with a TOF mass spectrometer, the source provides quantitative detection of elements in individual particles with mass amounts across six orders of magnitude, from 0.1 to 10'000 femtograms (fg) and mass concentrations ranging from 0.001 to 10'000 ng m-3 in a 30 s analysis. Here, we provide a description of the mipTOF, its performance characteristics, and operation of the instrument for direct ambient air analysis. As an example study, we provide selected results from a four-day continuous analysis of outdoor air.

## Instrument Design

In Figure 1, we provide a schematic of the mipTOF. The instrument consists of a MICAP plasma source (Radom Corp., USA), a water-cooled differentially pumped interface, an ion mirror to redirect the extracted ion beam and remove neutral species, an RF collision cell, an RF notch filter to selectively remove abundant ions of defined mass-to-charge (m/Q) values, and an orthogonal acceleration (oa) TOF mass analyzer. Typical operating parameters and specifications are provided in Tables 1 and 2. A support unit consisting of a nitrogen supply, a

rack-mount thermochiller, and a Roots pump required for instrument operation. Unlike a conventional Ar-sustained ICP source [13, 14], the MICAP can be operated with air directly injected into the central channel of the plasma. This enables the direct analysis of aerosol particles without the need for external gas-exchange or dilution devices [15, 16]. The mipTOF does not require cylinder-based gas supplies and is thus well suited for mobile or in-field analyses. During operation, the instrument consumes between 4.5-5.5 kWh of power depending on the plasma power selected.

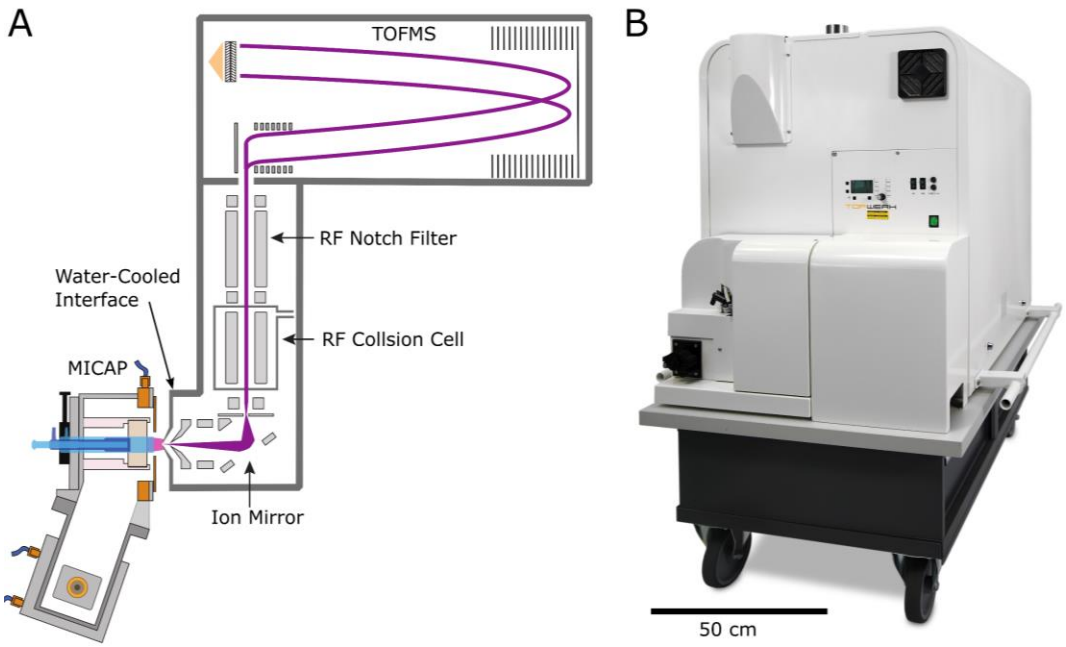


*Figure 1. A) Schematic diagram of the mipTOF. B) Image of the mipTOF instrument resting on top of a cart for mobile operation.*

*Table 1. Typical plasma operating parameters.*

| | |
|---|---|
| **Power** | 1250-1500 W |
| **Torch** | 1-piece Quartz, 1.5 mm injector diameter |
| **Outer Plasma Gas ($N_2$)** | 12.5 L/min |
| **Intermediate Plasma Gas ($N_2$)** | 1 L/min |
| **Central Plasma Gas ($N_2$)** | 1 L/min |

*Table 2. TOF mass analyzer specifications.*

| TOF Analyzer | |
|---|---|
| **Spectral Generation Rate** | 33 kHz |
| **Mass Range** | 7 –– 256 Th |
| **Mass Resolving Power** | 2000-3000 (m/Δm @ FWHM) |
| **Abundance Sensitivity** | < 100 ppm |
| **Dynamic Range** | $10^6$ |
| **Data Format** | Open-Source HDF5 |

## Aerosol Sampling and Detection Limits

Ambient air is sampled directly into the MICAP using a concentric pneumatic nebulizer as a Venturi pump, as shown in Figure 2.

The injection of air into the $N_2$ plasma does not destabilize the plasma or degrade instrument performance. Initial characterization of the mipTOF was achieved with the introduction of microdroplets with known element mass amounts of several elements. These microdroplets serve as particle proxies and allow the absolute calibration of the mipTOF, i.e. the counts recorded per unit mass of element injected into the plasma [17]. Typical detection limits for a range of elements are provided in Figure 3. These detection limits enable the effective detection of major elements in ultrafine particles (diameter < 100 nm) or the detection of minor and/or trace elements in larger particles (e.g. PM2.5). Particles with diameters up to ~5 um are expected to be completely vaporized and atomized in the plasma, and so the metal content of a broad range of particle sizes can be quantitatively measured [18].

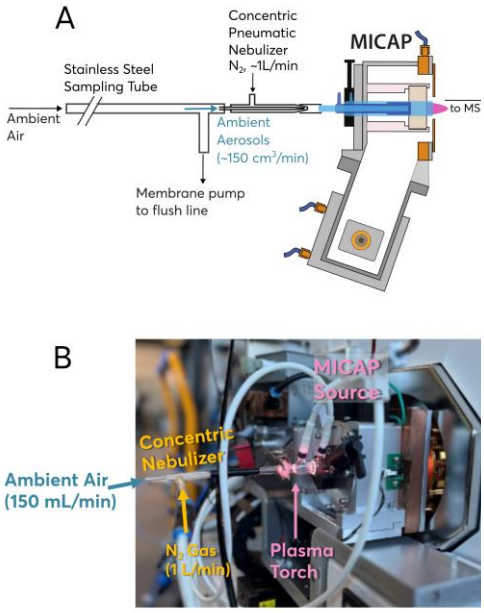


*Figure 2. A) Schematic of ambient aerosol sampling strategy using concentric pneumatic nebulizer as Venturi pump. B) Image of MICAP source in operation with direct ambient air sampling through concentric nebulizer.*

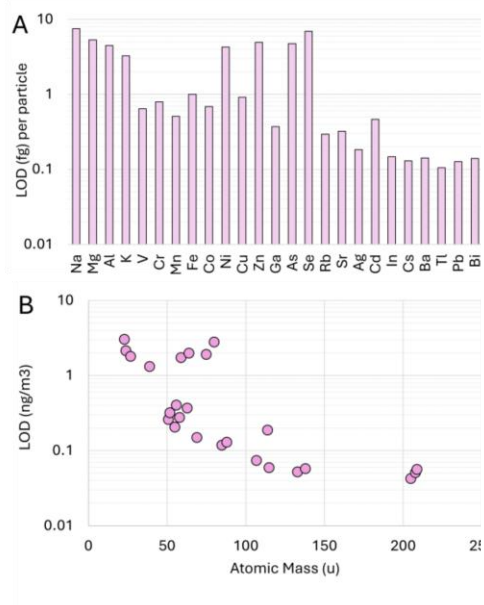


*Figure 3. A) Per particle detection limits of the mipTOF. B) Bulk concentration LODs of the mipTOF measured in 10 s.*

### Continuous Four-Day Ambient Air Measurement

To assess the mipTOF's capability for air monitoring, we performed a semi-continuous measurement of ambient air between 22:00 on Friday, Oct 25 to Wednesday, Oct 30, 2024, at 1:00. Air was sampled with a diaphragm pump at a flow rate of 3 L/min from the fourth floor of the TOFWERK laboratory in Thun, Switzerland through an 11-m long, 10-mm diameter stainless steel tube. Prior to the sampled air reaching the membrane pump, the air flow was subsampled with a pneumatic nebulizer at a flow rate of 150 mL/min. Element mass concentrations were determined with the online microdroplet calibration method [17] and data were processed in TOF-SPI [19]. A workflow diagram of the data processing procedure is given in Figure 4. Data were collected in 95 files; each TOF acquisition was 62 min in duration with a average spectral generation rate of 200 Hz (5 ms/spectrum). One-minute-long bursts of microdroplets (20 Hz, ~63 pL/droplet) were applied at the start and end of each measurement and 1-hour of aerosol-only measurement time was between the droplets. The droplet signals were used to determine the elemental sensitivities in counts/fg and then to determine element mass amounts per aerosol particle. In Table 3, we provide average data from the droplet standards and for the measurement period of the metal aerosols. Consecutive data were collected with a gap of ~3.5 minutes, so when accounting for the droplet calibration regions, each sequential one-hour aerosol measurement had a gap of ~5.5 min.

Following initial processing of the mipTOF data, the average mass concentrations in five-minute time windows across the entire measurement period were assembled. In Figure 5, the determined particle-resolved mass concentrations for select elements are plotted. As seen, the metal concentrations recorded from the ambient air vary across several orders of magnitude and are highly time dependent. For example, when considering the time traces of magnesium and calcium, metal concentration elevations are clearly correlated with the start of the work week (i.e. Monday Oct. 28) and with daytime working hours. On the other hand, some elements such as iron, manganese, and lead, are present at low levels continuously but also appear as sharp increases in concentration at specific times.

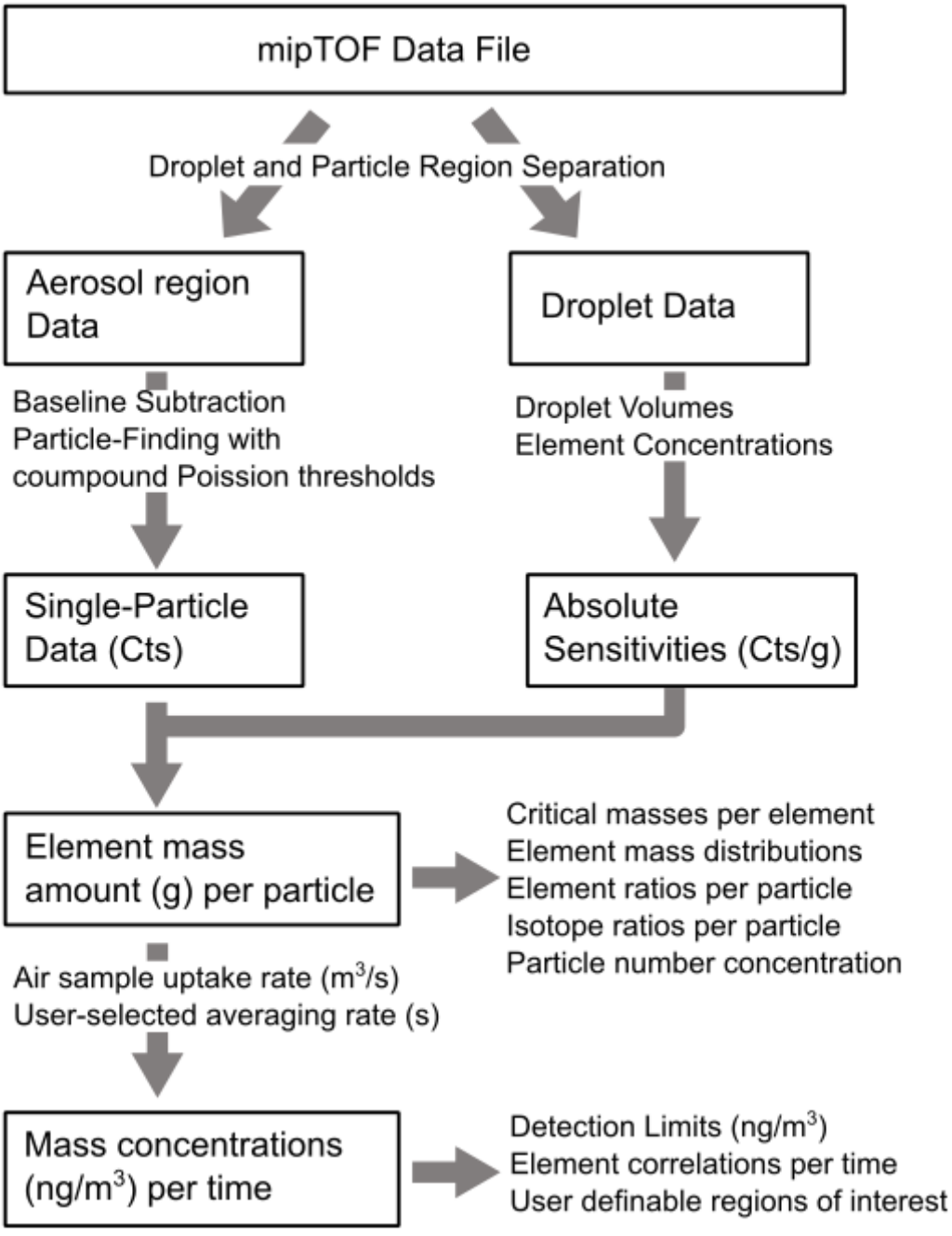


*Figure 4. Workflow diagram of data-processing for particle-resolved element mass amount calibration and average mass concentration determinations.*

*Table 3. Droplet Calibration: average signals, sensitivities, and critical masses.*

| Element | Isotopes Used | Avg Droplet Signal (Cts) | Sensitivity (Cts/fg) | Critical Mass (fg) |
|---|---|---|---|---|
| Na | $^{23}$Na | 18.0 | 0.56 ± 0.06 | 14 ± 2 |
| Mg | $^{24}$Mg | 12.1 | 0.41 ± 0.03 | 16 ± 2 |
| Al | $^{27}$Al | 18.5 | 0.60 ± 0.05 | 11 ± 1 |
| K | $^{39}$K | 57.4 | 1.7 ± 0.2 | 7 ± 1 |
| Ca | $^{40}$Ca | 66.5 | 1.6 ± 0.2 | 24 ± 5 |
| V | $^{51}$V | 95.0 | 3.0 ± 0.3 | 2.4 ± 0.2 |
| Cr | $^{52}$Cr | 66.4 | 2.2 ± 0.2 | 3.2 ± 0.3 |
| Mn | $^{55}$Mn | 119.6 | 3.8 ± 0.3 | 1.7 ± 0.2 |
| Fe | $^{56}$Fe | 82.6 | 2.6 ± 0.2 | 2.3 ± 0.3 |
| Co | $^{59}$Co | 63.9 | 2.1 ± 0.2 | 3.4 ± 0.3 |
| Ni | $^{60}$Ni | 13.1 | 0.44 ± 0.03 | 17 ± 2 |
| Cu | $^{63}$Cu + $^{65}$Cu | 41.5 | 1.3 ± 0.1 | 5.2 ± 0.6 |
| Zn | $^{66}$Zn | 3.7 | 0.25 ± 0.01 | 28 ± 2 |
| Ga | $^{71}$Ga | 61.8 | 2.0 ± 0.1 | 3.4 ± 0.3 |
| Sr | $^{88}$Sr | 269.1 | 8.4 ± 0.9 | 0.9 ± 0.1 |
| Y | $^{89}$Y | 247.4 | 7.2 ± 0.8 | 1.0 ± 0.1 |
| Ag | $^{107}$Ag + $^{109}$Ag | 234.4 | 7.2 ± 0.7 | 1.0 ± 0.1 |
| Cd | $^{111}$Cd | 13.7 | 0.45 ± 0.03 | 15 ± 1 |
| In | $^{115}$In | 352.6 | 11 ± 1 | 0.62 ± 0.06 |
| Ba | $^{138}$Ba | 485.8 | 15 ± 2 | 0.47 ± 0.07 |
| Ce | $^{140}$Ce | 525.1 | 17 ± 2 | 0.45 ± 0.05 |
| Tl | $^{203}$Tl + $^{205}$Tl | 691.6 | 21 ± 2 | 0.34 ± 0.04 |
| Pb | $^{206}$Pb + $^{207}$Pb + $^{208}$Pb | 653.3 | 20 ± 2 | 0.37 ± 0.05 |
| Bi | $^{209}$Bi | 515.1 | 16 ± 2 | 0.42 ± 0.05 |
| U | $^{238}$U | 633.3 | 85 ± 10 | 0.34 ± 0.04 |

With mipTOF analysis, element concentration data can be interrogated at different timescales: from a time resolution of milliseconds, at which elements in individual particles are resolved, to a time resolution of minutes or longer. The improved time resolution of mipTOF aerosol detection compared to bulk analysis of metal aerosols enables better analysis of element covariation, which can be used for source apportionment [20, 21] with established approaches such as positive matrix factorization [22, 23]. For example, in Figure 5, the striking correlation of elevated Mn and Fe mass concentrations at ~4:00 in the morning on Oct. 28 indicates that these elements come from a common particle source. Speculatively, we attribute these particles to overnight train-track maintenance (e.g. track grinding), as the train tracks are around 25 m from the sampling position. The high-resolution data multi-elemental concentration information offered by mipTOF analysis should also allow for one to account for wind velocity and use concentration-weighted trajectory analysis [24, 25] to better pinpoint source emitters.

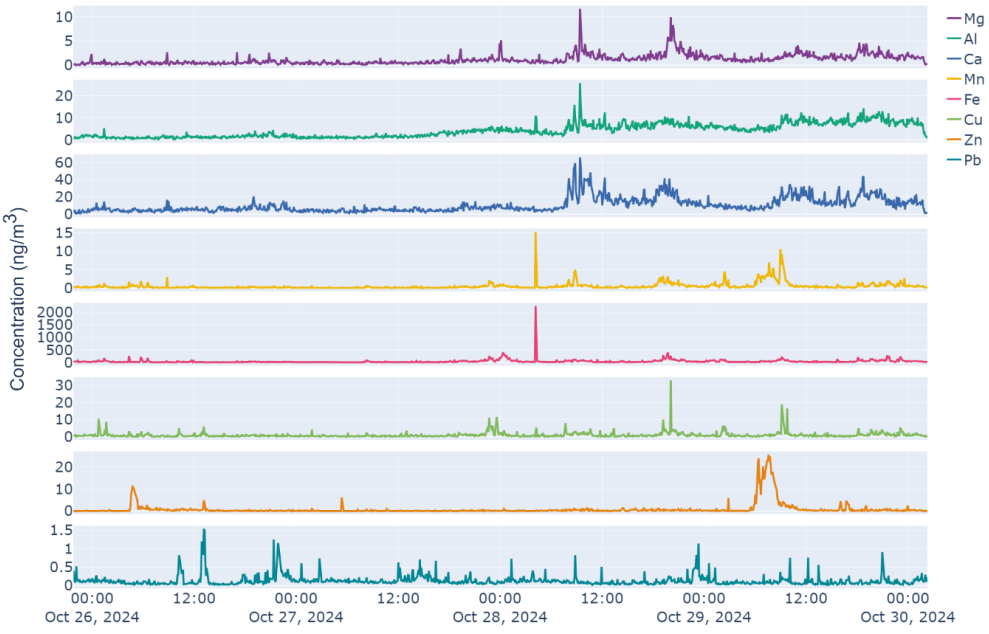


*Figure 5. Average concentrations (ng/m3) recorded across five-minute measurement windows for select elements. Data were collected for four days at a base time resolution of 5 ms/spectrum. At this time resolution, element mass amounts in individual particles can be determined and average mass concentrations at time scales from seconds to minutes can be evaluated.*

### Analysis of Metal Aerosols: Particle-Resolved Data for Elemental Fingerprinting

To highlight the depth of data available from mipTOF ambient air analysis, we consider two example time periods of interest from the acquired data. In Figure 6, we plot the time-averaged mass concentrations of lead particles and select data from a 30 min period at around noon on Saturday Oct. 26. This time period represents the highest concentration of lead recorded across our measurements. For any time region of interest, particle-resolved data can be extracted from the mipTOF dataset. In the 30 min period highlighted in Figure 6A, over 3000 metal-containing aerosol particles were recorded; 1170 of these particles contained Pb. In Fig. 6B, we plot the correlation of the mass amounts of Pb-208 and Pb-206 determined from the individual Pb-containing particles. As seen, Pb isotope ratios recorded in the particles follow the average natural abundance of Pb isotopes on earth [26]. The scatter in determined Pb ratios from individual metal aerosols is due to Poisson statistics [27], and the constrained ratio indicates that outlier Pb-isotope ratios from, e.g., thorogenic mineral dust [28] could be identified at the single-particle level and used for improved source apportionment. In Figure 6C, we plot the overall particle composition (i.e. the determined element mass amounts) of 1000 randomly selected particle events from the Pb-rich region of interest. As seen, the second and third most commonly detected element in these particles are Fe and Ba, respectively. By plotting the mean mass amount of each element, a unique element fingerprint of particles from this time region of interest can be developed; this average element fingerprint is shown above the heatmap.

### Analysis of Metal Aerosols: Particle Composition for Source Apportionment

In a second example, we explore the particle composition from a 15 min period at ~4:00 in the morning on Monday Oct. 28. This time period of interest is highlighted in Figure 7A, and consists of elevated amounts of Fe, Mn, Cr, and Zr. In this time period, over 13000 particles were recorded, which is the highest particle flux recorded across the four days. Of this particle population, 12145 of the particles contained Fe and 2194 particles had measurable amounts of Fe, Mn, and Cr. In Figure 7B, we plot the correlation of Fe and Mn. As seen, the central ratio of Fe:Mn in the particles is ~120:1; however, the scatter in the element ratio is quite broad, with Fe:Mn ratios of more than 500:1 and less than 25:1.

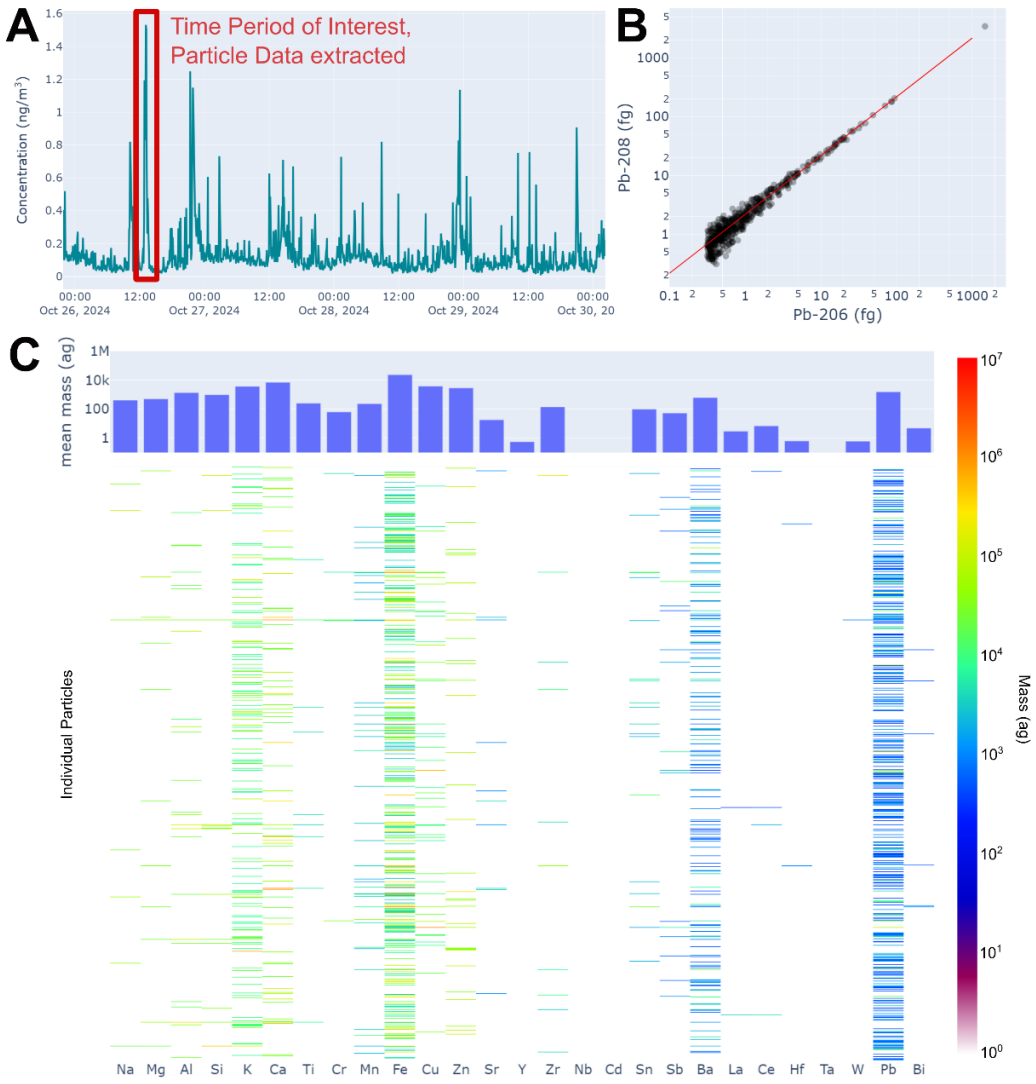


*Figure 6. A) Average concentrations of Pb across the whole mipTOF measurement duration. The time period with the highest concentration of Pb is highlighted and the isotope correlation of Pb-206 and Pb-208 in individual particles from this time period is provided in B. The red line in B is the correlation expected from the average natural Pb isotope abundances on earth, i.e. 2.17:1, 208Pb:206Pb. C) Heat map of element mass amounts recorded from 1000 randomly selected particles from the time period of interest. Each row of the heatmap provides the masses of elements recorded for an individual particle. Elements not detected in a given particle are plotted in white and the log of the mass amounts of the elements is plotted on the false-color scale. Above the heatmap, the average mass amounts of each element in all particles in the time period of interest is given as a bar graph.*

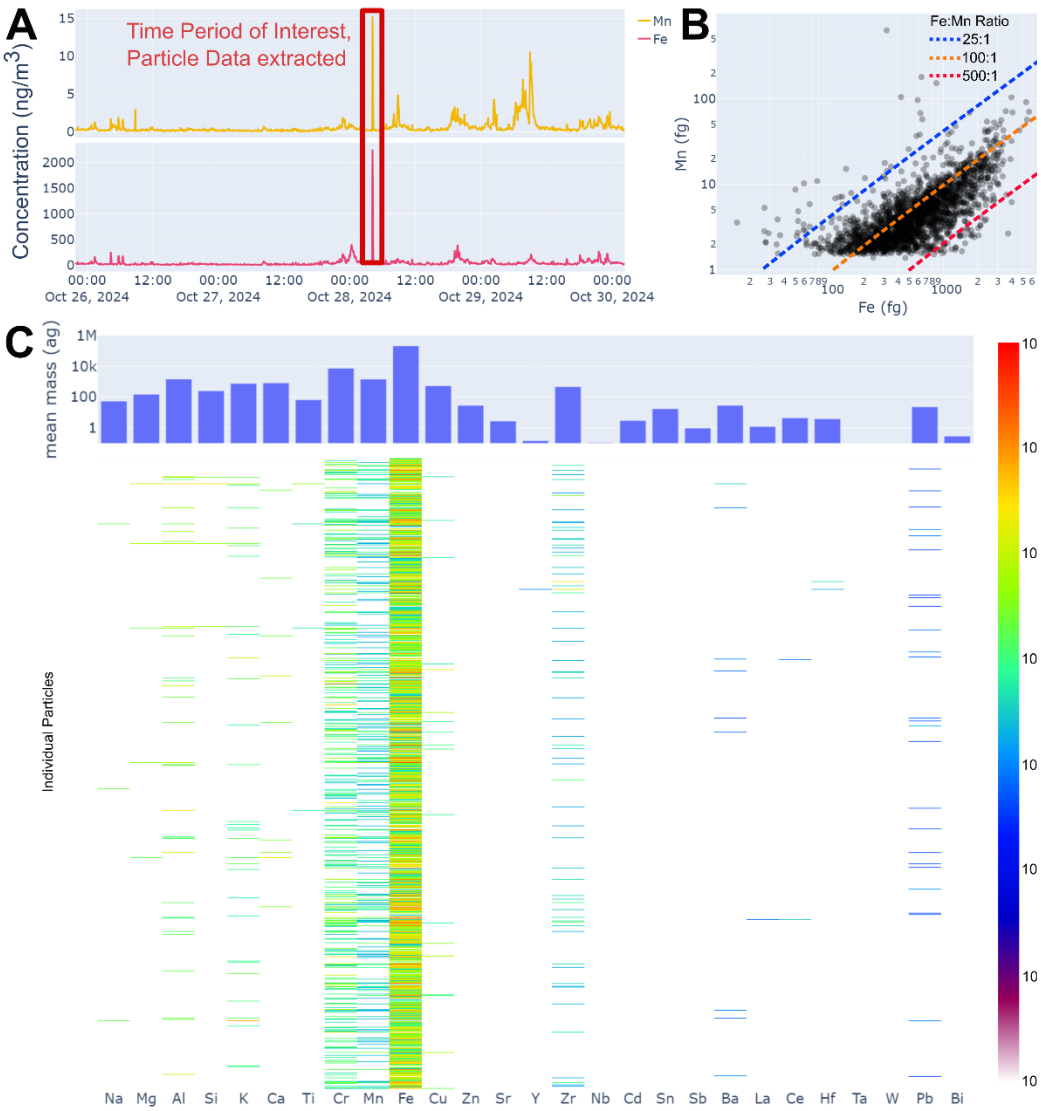


*Figure 7. A) Average concentrations of Mn and Fe across the whole mipTOF measurement duration. The time period with the highest concentration of Fe and Mn is highlighted and the element correlation of Mn vs. Fe in individual particles from this time period is provided in B. C) Heat map of element mass amounts recorded from 1000 randomly selected particles from the time period of interest. Each row of the heatmap provides the masses of elements recorded for an individual particle. Elements not detected in a given particle are plotted in white and the log of the mass amounts of the elements is plotted on the false-color scale. Above the heatmap, the average mass amounts of each element in all particles in the time period of interest is given as a bar graph.*

This spread in the element ratios cannot be accounted for by Poisson statistics, and so is the result of heterogeneity in the element composition of the particles. The Fe:Mn ratio recorded is consistent with 1084 hot-rolled steel often used for railway tracks, which has a Mn mass fraction from 0.6-1%. In Figure 7C, we plot the overall particle composition (i.e. the determined element mass amounts) of 1000 randomly selected particle events from the Fe-Mn-Cr-rich time period of interest. Above the heatmap, we plot the average element mass amount per particle. As seen by both the heatmap and the element-mass fingerprint, the composition of particles in this Fe-Mn-Cr rich region is very different than that in Pb-rich region from Figure 6. The particles in the Fe-Mn-Cr-rich region generally have a much higher Fe, Mn, Cr, and Zr content; likewise, the Pb and Ba content is much lower than that in the Pb-rich region. These differences in particle population composition indicate different relative contributions from sources in the two time regions. In the future, use of advanced data analysis tools, such as positive matrix factorization, should enable time-resolved unmixing of sources from mipTOF data.

## Conclusion

The mipTOF is a new trace-element mass spectrometer that can be used for the direct quantitative analysis of metals and metalloids in air. The high sensitivity of the mipTOF enables particle-resolved quantification of elements with absolute detection limits in the range of 100 s of attograms to 10 s of femtograms per particle. With the mipTOF, highly time resolved metal aerosol concentrations can be determined, which expands the use of metal aerosols for source apportionment. The instrument's simple operational requirements – needing only a power source without the need for compressed gases – make it particularly valuable for extended field campaigns and continuous monitoring. The combination of high sensitivity, temporal resolution, and field durability positions the mipTOF as a promising tool for advancing the understanding of metal aerosol dynamics and improving air quality monitoring capabilities.

## Contact

sales@tofwerk.com

## References


[1] W. H. Zoller, et. al. "Atmospheric Concentrations and Sources of Trace Metals at the South Pole." Science, 183, 198-200, 1974.

[2] O. Ramírez, et. al. "Hazardous trace elements in thoracic fraction of airborne particulate matter: Assessment of temporal variations, sources, and health risks in a megacity." Science of The Total Environment, 710, 136344, 2020.

[3] Y. Suzuki, et. al. "Determination of Rare Earth Elements (REEs) in Airborne Particulate Matter (APM) Collected in Tokyo, Japan, and a Positive Anomaly of Europium and Terbium." Analytical Sciences, 26, 929-935, 2010.

[4] F. Drewnick, et. al. "A New Time-of-Flight Aerosol Mass Spectrometer (TOF-AMS)—Instrument Description and First Field Deployment." Aerosol Science and Technology, 39, 637-658, 2005.

[5] T. M. Ruuskanen, et. al. "Eddy covariance VOC emission and deposition fluxes above grassland using PTR-TOF." Atmos. Chem. Phys., 11, 611-625, 2011.

[6] K. A. Pratt and K. A. Prather. "Mass spectrometry of atmospheric aerosols—Recent developments and applications. Part II: On-line mass spectrometry techniques." Mass Spectrometry Reviews, 31, 17-48, 2012.

[7] M. Furger, et. al. "Elemental composition of ambient aerosols measured with high temporal resolution using an online XRF spectrometer." Atmos. Meas. Tech., 10, 2061-2076, 2017.

[8] C. A. Noble and K. A. Prather. "Real-time single particle mass spectrometry: A historical review of a quarter century of the chemical analysis of aerosols." Mass Spectrometry Reviews, 19, 248-274, 2000.

[9] A. R. Jensen, et. al. "Measurements of volatile organic compounds in ambient air by gas-chromatography and real-time Vocus PTR-TOF-MS: calibrations, instrument background corrections, and introducing a PTR Data Toolkit." Atmos. Meas. Tech., 16, 5261-5285, 2023.

[10] M. Rutherford, et. al. "Mobile VOC measurements in Commerce City, CO reveal the emissions from different sources." Journal of the Air & Waste Management Association, 74, 714-725, 2024.

[11] A. J. Schwartz, et. al. "New inductively coupled plasma for atomic spectrometry: the microwave-sustained, inductively coupled, atmospheric-pressure plasma (MICAP)." Journal of Analytical Atomic Spectrometry, 31, 440-449, 2016.

[12] M. Schild, et. al. "Replacing the Argon ICP: Nitrogen Microwave Inductively Coupled Atmospheric-Pressure Plasma (MICAP) for Mass Spectrometry." Analytical Chemistry, 90, 13443-13450, 2018.

[13] H. Niu and R. S. Houk. "Fundamental aspects of ion extraction in inductively coupled plasma mass spectrometry." Spectrochimica Acta Part B: Atomic Spectroscopy, 51, 779-815, 1996.

[14] R. S. Houk, et. al. "Inductively coupled argon plasma as an ion source for mass spectrometric determination of trace elements." Analytical Chemistry, 52, 2283-2289, 1980.

[15] K. Nishiguchi, et. al.. "Real-time multielement monitoring of airborne particulate matter using ICP-MS instrument equipped with gas converter apparatus." Journal of Analytical Atomic Spectrometry, 23, 1125-1129, 2008.

[16] T. Cen, et. al. "Rotating disk diluter hyphenated with single particle ICP-MS as an online dilution and sampling platform for metallic nanoparticles characterization in ambient aerosol." Journal of Aerosol Science, 175, 106283, 2024.
[17] K. Mehrabi, et. al. "Single-particle ICP-TOFMS with online microdroplet calibration for the simultaneous quantification of diverse nanoparticles in complex matrices." Environmental Science: Nano, 6, 3349-3358, 2019.
[18] T. Van Acker, et. al. "Laser Ablation for Nondestructive Sampling of Microplastics in Single-Particle ICP-Mass Spectrometry." Analytical Chemistry, 95, 18579-18586, 2023.
[19] A. Gundlach-Graham, et. al. "Introducing "time-of-flight single particle investigator" (TOF-SPI): a tool for quantitative spICP-TOFMS data analysis." Journal of Analytical Atomic Spectrometry, 39, 704-711, 2024.
[20] S. Giannoukos, et. al. "Real-time detection of aerosol metals using online extractive electrospray ionization mass spectrometry." Analytical chemistry, 92, 1316-1325, 2019.
[21] Y. Suzuki, et. al. "Assignment of PM2.5 sources in western Japan by non-negative matrix factorization of concentration-weighted trajectories of GED-ICP-MS/MS element concentrations." Environmental Pollution, 270, 116054, 2021.
[22] P. Paatero and U. Tapper. "Positive matrix factorization: A non-negative factor model with optimal utilization of error estimates of data values." Environmetrics, 5, 111-126, 1994. https://doi.org/10.1002/env.3170050203
[23] Y. Song, et. al. "Source apportionment of PM2.5 in Beijing by positive matrix factorization." Atmospheric Environment, 40, 1526-1537, 2006.
[24] Y.-K. Hsu, et. al. "Comparison of hybrid receptor models to locate PCB sources in Chicago." Atmospheric Environment, 37, 545-562, 2003.
[25] C. A. Brereton and M. R. Johnson. "Identifying sources of fugitive emissions in industrial facilities using trajectory statistical methods." Atmospheric Environment, 51, 46-55, 2012.